Electronically excited states of water clusters of 7-azaindole: Structures, relative energies, and electronic nature of the excited states

Yuriy N. Svartsov and Michael Schmitt

Citation: J. Chem. Phys. **128**, 214310 (2008); doi: 10.1063/1.2928636
View online: http://dx.doi.org/10.1063/1.2928636
View Table of Contents: http://jcp.aip.org/resource/1/JCPSA6/v128/i21
Published by the American Institute of Physics.

Additional information on J. Chem. Phys.

Journal Homepage: http://jcp.aip.org/
Journal Information: http://jcp.aip.org/about/about_the_journal
Top downloads: http://jcp.aip.org/features/most_downloaded
Information for Authors: http://jcp.aip.org/authors

ADVERTISEMENT

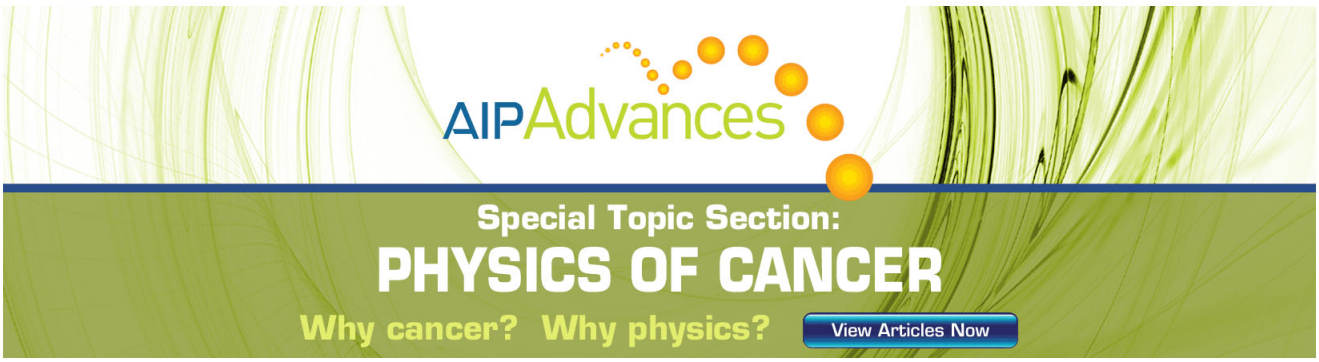

Downloaded 24 Apr 2012 to 134.99.152.12. Redistribution subject to AIP license or copyright; see http://jcp.aip.org/about/rights_and_permissions

Electronically excited states of water clusters of 7-azaindole: Structures, relative energies, and electronic nature of the excited states

Yuriy N. Svartsov[1] and Michael Schmitt[2,a)]
[1]*Institut für Anorganische Chemie, Johannes Kepler Universität Linz, Altenbergerstraße 69, A-4040 Linz, Austria*
[2]*Institut für Physikalische Chemie I, Heinrich-Heine-Universität, D-40225 Düsseldorf, Germany*

(Received 1 February 2008; accepted 23 April 2008; published online 6 June 2008)

The geometries of 1*H*-7-azaindole and the 1*H*-7-azaindole$(H_2O)_{1-2}$ complexes and the respective 7*H* tautomers in their ground and two lowest electronically excited $\pi-\pi^*$ singlet states have been optimized by using the second-order approximated coupled cluster model within the resolution-of-the-identity approximation. Based on these optimized structures, adiabatic excitation spectra were computed by using the combined density functional theory/multireference configuration interaction method. Special attention was paid to comparison of the orientation of transition dipole moments and excited state permanent dipole moments, which can be determined accurately with rotationally resolved electronic Stark spectroscopy. The electronic nature of the lowest excited state is shown to change from L_b to L_a upon water complexation. © *2008 American Institute of Physics*. [DOI: 10.1063/1.2928636]

I. INTRODUCTION

Azaindole has two possible sites for hydrogen bonding one potentially acting as proton donor and the other as proton acceptor. This behavior, which is shared with chromophores such as 2-pyridone,[1] 7-hydroxyquinoline,[2] and 1*H*-pyrrolo[3,2-*h*] quinoline,[3] opens the possibility to form chains of water molecules bridging the two binding sites. Since azaindole may exist in two tautomeric forms, 1*H*-7-azaindole (1*H*-pyrrolo[2,3-b]pyridine) and 7*H*-7-azaindole (7*H*-pyrrolo[2,3-b]pyridine) (cf. Fig. 1), these water chains may be capable of inducing a proton transfer which interconverts the two tautomeric forms. The relative energies of the two tautomers depend strongly on the number of water molecules in the chain and on the electronic state. In the following, we will study the 7-azaindole$(H_2O)_1$ and the 7-azaindole$(H_2O)_2$ clusters, which will be called the 1:1 and the 1:2 clusters, respectively.

Relative stabilities of 7-azaindole and its water and methanol complexes in the ground and first excited singlet states were studied by Gordon.[4] He found that the relative stabilities of the tautomers of 7-azaindole and the 7-azaindole-water complex are reversed upon electronic excitation, the 7*H* tautomer being the more stable one in the excited state.

Shukla and Mishra studied the effect of solvation on the ordering of low-lying excited singlet states of 7-azaindole and its tautomer by using configuration interaction involving singly excited configurations.[5] They found the second electronically excited S_2 state of 7-azaindole to be of $(n\text{-}\pi^*)$ character, while it is $(\pi\text{-}\pi^*)$ type upon water interaction.

The absorption and emission spectra of 7-azaindole have been studied theoretically by Borin and Serrano-Andrés by using the complete active space (CAS) self-consistent field (SCF) method and multiconfigurational second-order perturbation theory.[6,7]

Casadesús *et al.* investigated the proton transfer in the ground and excited states of isolated 7-azaindole-water complexes by using time dependent density functional theory (TDDFT).[8] A concerted but nonsynchronous tautomerism mechanism was predicted. The barrier for tautomerization has been shown to decrease upon electronic excitation and with cluster size.

Fernández-Ramos *et al.* calculated potential energy surfaces of several azaindole-water complexes at the CASSCF(8,8) level.[9] Optimization of the cluster structures in a spherical solvent cavity yielded potential energy surfaces on which temperature-dependent multidimensional proton transfer rate constants were calculated. While for the isolated 1:1 and 1:2 clusters, no fast proton transfer was observed, a second solvation shell of three additional water molecules in the 1:2 cluster greatly enhances the proton transfer rate, while addition of four molecules in the second solvation shell to the 1:1 cluster has no comparable effect.

On the experimental side, Nakajima *et al.*[10] investigated the geometric structures of 7-azaindole$(H_2O)_{1-3}$ and of the 7-azaindole dimer by using laser-induced fluorescence spectroscopy with high resolution ($\sim$0.01 cm^{-1}, equivalent to 300 MHz). They deduced a planar structure of 7-azaindole$(H_2O)_1$ from the rotational analysis of the spectrum.

Yokoyama *et al.* performed IR dip spectroscopy on 7-azaindole water clusters together with *ab initio* molecular orbital calculations.[11] From their results, hydrogen bonded single ring structures for the 7-azaindole$(H_2O)_n$ with $n=1-3$ clusters was deduced.

The structural changes of the azaindole$(H_2O)_1$ cluster upon electronic excitation were determined from a Franck–

a)Electronic mail: mschmitt@uni-duesseldorf.de. Tel.: +49 211 81 12100. FAX: +49 211 81 15195.

 © 2008 American Institute of Physics

Downloaded 24 Apr 2012 to 134.99.152.12. Redistribution subject to AIP license or copyright; see http://jcp.aip.org/about/rights_and_permissions

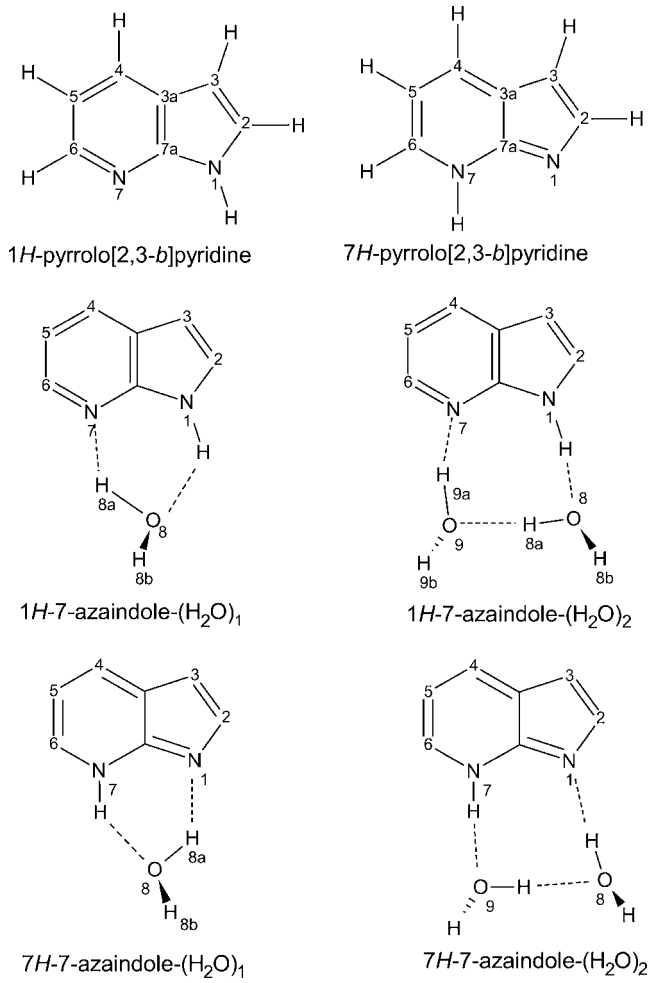

FIG. 1. Structures and atomic numbering of the two 7-azaindole tautomers and their $n=1,2$ water clusters.

Condon analysis of the emission spectra obtained via pumping of several vibronic bands.[12] Both the O···H and the H···N hydrogen bond lengths are found to decrease upon electronic excitation, accompanied by a distortion of the monomer geometry.

The geometrical changes of the 7-azaindole monomer itself were investigated by using rotationally resolved electronic spectroscopy of four different isotopomers of 7-azaindole[13] as well as a Franck–Condon analysis.[14] In the former study, the nature of the electronically excited state has been shown to be of L_b character. Recently, the excited state dipole moment of 7-azaindole has been determined by Kang *et al.* from the Stark effect in a rotationally resolved laser-induced fluorescence spectrum.[15]

The present publication attempts to explain the experimental findings in a parallel experimental study on the excited states of the $n=1$ and 2 water clusters of 7-azaindole. These results are presented in the accompanying study by Vu *et al.*[16]

II. COMPUTATIONAL METHODS

Structure optimizations were performed by employing the valence triple zeta basis set with polarization functions (d,p) from the TURBOMOLE library.[17,18] The equilibrium geometries of the electronic ground and the lowest excited singlet states were optimized at the levels of DFT and TDDFT.[19,20] The B3-LYP functional was used.[21] Additional optimizations were performed with the approximate coupled cluster singles and doubles model (CC2) by employing the resolution-of-the-identity approximation (RI).[22–24] First order transition states were preoptimized at the B3-LYP level with the 6-31G(d,p) basis set by using the QST3 method[25] as implemented in the GAUSSIAN03 program package.[26] With the so obtained structures as basis, the transition state structures were optimized at the RICC2 level by using the TRIM (trust radius image minimization) method[27] implemented in the STATPT module from TURBOMOLE V5.8 for the S_0 and the S_1 states with the same basis sets as for the minimum structures.

The singlet state energies and wave functions were calculated by using the combined DFT/multireference configuration interaction (DFT/MRCI) method by Grimme and Waletzke.[28] The configuration state functions (CSFs) in the MRCI expansion are constructed from Kohn-Sham (KS) orbitals, optimized for the dominant closed shell determinant of the electronic ground state employing the BH-LYP (Refs. 29 and 30) functional. All valence electrons were correlated in the MRCI runs [62 for the 7-azaindole monomer, 72 for the 7-azaindole$(H_2O)_1$ cluster, and 82 for the 7-azaindole$(H_2O)_1$ cluster] and the eigenvalues and eigenvectors of four singlet states were determined. The *initial* set of reference CSFs was generated automatically in a CAS type procedure (including all single and double excitations from the five highest occupied molecular orbitals in the KS determinant to the five lowest virtual orbitals) and was then iteratively improved. The MRCI expansion was kept moderate by extensive configuration selection. The selection of the most important CSFs is based on an energy gap criterion as described in Ref. 28. Only those configurations with an energy below a certain cutoff energy were taken into account. The energy of a given configuration was estimated from orbital energies within the selection procedure. The cutoff energy was given by the energy of the highest desired root as calculated for the reference space plus a cutoff parameter $\delta E_{\mathrm{sel}}=1.0E_H$. The latter choice has been shown to yield nearly converged results in Ref. 28. The so obtained MRCI space was spanned by about 70 000 CSFs from approximately 138 reference configurations.

III. RESULTS

The structures of the 7-azaindole monomer and of the 7-azaindole$(H_2O)_n$ clusters with $n=1,2$ were optimized at B3-LYP/TZVP level for the electronic ground state and at the TD B3-LYP/TZVP level for the first and second electronically excited singlet states. Subsequently, the so obtained structures were reoptimized at the RICC2/TZVP level for the ground state and the lowest electronically excited singlet states. Table I compares the rotational constants, calculated at the TD B3-LYP level for S_0, S_1, and S_2 states, respectively. Analysis of the main orbital contributions to the excitations shows the S_1 states of 7-azaindole and of 7-azaindole$(H_2O)_{1,2}$ to be of L_a character [mainly highest occupied molecular orbital (HOMO) to lowest unoccupied

Downloaded 24 Apr 2012 to 134.99.152.12. Redistribution subject to AIP license or copyright; see http://jcp.aip.org/about/rights_and_permissions

TABLE I. Rotational constants (in MHz) of the S_0, S_1, and S_2 states, calculated at the (TD-)B3-LYP/TZVP level of theory. The values in parentheses give the experimentally determined rotational constants from Ref. 13 for the monomer and from Ref. 16 for the $n=1$ and 2 water clusters.

State	Species	A (MHz)	B (MHz)	C (MHz)
S_0	7-AI	3955(3929)	1704(1703)	1191(1188)
	7-AI$(H_2O)_1$	1768(1762)	1355(1343)	768(763)
	7-AI$(H_2O)_2$	1424(1414)	856(828)	537(524)
S_1	7-AI	3906	1672	1171
	7-AI$(H_2O)_1$	1793(1798)	1369(1358)	777(775)
	7-AI$(H_2O)_2$	1393(1423)	824(855)	521(537)
S_2	7-AI	3774(3745)	1704(1704)	1174(1172)
	7-AI$(H_2O)_1$	1772	1335	762
	7-AI$(H_2O)_2$	1416	831	527

MO (LUMO) excitation, large dipole moment], while the S_2 states shows strong mixing and are composed of HOMO −1 to LUMO and HOMO to LUMO+1 excitations, with a small dipole moment, typical for a L_b state. Comparison of the experimental rotational constants from Ref. 16 (shown in parentheses in Table I) with the calculated ones shows that in the case of the 7-azaindole monomer, the observed excited state is the L_b state, and in the case of both 7-azaindole-water clusters, the L_a state. Nevertheless, at this level of theory, the experimentally observed state of the monomer is adiabatically the second excited singlet state.

While it has been shown that structures of electronically excited states are quite reliably predicted at the level of TD-DFT, the relative energies of the excited states and their exact geometry are more accurately described by the RICC2 model. In the following, we performed RICC2 calculations on the electronic ground state and the L_b state for the 7-azaindole monomer and the L_a state for the 7-azaindole-water clusters, which are both the lowest excited singlet states at this level of theory in contrast to the TD DFT calculations (*vide supra*). Both the 1*H* and 7*H* tautomeric forms (cf. Fig. 1) have been considered for 7-azaindole and its water clusters. The ground states of the 1*H* and 7*H* tautomers have been calculated by assuming C_s symmetry, while no symmetry constraints were made for the excited states and for the 7-azaindole-water clusters (cf. Tables II and III).

TABLE II. Rotational constants, S_0 and S_1 state geometry parameters of 1*H* tautomer of 7-azaindole and of the 7-azaindole$(H_2O)_{1,2}$ clusters, calculated at the RICC2/TZVP level of theory. Experimental values are given in parentheses for the monomer from Ref. 13 and for the $n=1$ and 2 water clusters from Ref. 16. For the atomic numbering, refer to Fig. 1. All bond lengths are given in pm, and angles and dihedral angles are given in deg.

	S_0			S_1		
1*H* tautomer	7-AI	7-AI$(H_2O)_1$	7-AI$(H_2O)_2$	7-AI	7-AI$(H_2O)_1$	7-AI$(H_2O)_2$
A (MHz)	3918	1784	1425	3737	1819	1430
	(3929)	(1762)	(1414)	(3746)	(1798)	(1423)
B (MHz)	1704	1353	842	1694	1367	842
	(1703)	(1343)	(828)	(1704)	(1358)	(855)
C / MHz	1187	771	533	1166	782	533
	(1188)	(763)	(524)	(1172)	(775)	(537)
ΔI (amu Å^2)	0.00	−1.04	−6.68	0.00	−1.04	−13.10
N_1C_2	138.0	137.7	137.8	141.8	132.9	133.1
C_2C_3	137.6	137.8	137.8	137.5	143.5	143.1
C_3C_{3a}	142.9	142.8	142.6	143.6	144.0	144.2
$C_{3a}C_{7a}$	142.5	142.6	142.9	145.2	138.8	138.8
$C_{7a}N_1$	137.4	137.0	136.9	135.3	144.1	144.2
$C_{3a}C_4$	140.1	140.0	139.9	142.3	143.1	143.0
C_4C_5	139.1	139.2	139.2	142.8	142.3	142.2
C_5C_6	140.6	140.4	140.3	143.4	138.4	138.3
C_6N_7	134.3	134.4	134.5	137.5	140.9	141.1
N_7C_{7a}	133.6	134.2	134.2	136.3	134.5	134.8
N_1H_1	101.0	101.8	103.1	101.3	103.9	105.9
O_8H_{8a}	⋯	98.0	98.5	⋯	99.7	99.8
O_8H_{8b}	⋯	96.3	96.3	⋯	96.3	96.4
H_1O_8	⋯	198.6	178.3	⋯	178.1	162.1
N_7H_{8a}	⋯	195.3	⋯	⋯	179.5	⋯
$N_1H_1O_8$	⋯	135	172	⋯	138	171
$N_7H_{8a}O_8$	⋯	147	⋯	⋯	149	⋯
$N_1H_1O_8H_{8b}$	⋯	113	126	⋯	120	148
N_7H_{9a}	⋯	⋯	181.0	⋯	⋯	167.6
$N_7H_{9a}O_9$	⋯	⋯	171	⋯	⋯	170
$N_7H_{9a}O_9H_{9b}$	⋯	⋯	−122	⋯	⋯	−123
O_9H_{8a}	⋯	⋯	173.7	⋯	⋯	163.8
$O_9H_{8a}O_8$	⋯	⋯	162	⋯	⋯	163

Downloaded 24 Apr 2012 to 134.99.152.12. Redistribution subject to AIP license or copyright; see http://jcp.aip.org/about/rights_and_permissions

TABLE III. S_0 and S_1 state geometry parameters of the 7*H* tautomer of 7-azaindole and of the 7-azaindole$(H_2O)_{1,2}$ clusters, optimized at the RICC2/TZVP level of theory. For the atomic numbering, refer to Fig. 1. All bond lengths are given in pm, and angles and dihedral angles are given in deg.

	S_0			S_1		
7*H* tautomer	7-AI	7-AI$(H_2O)_1$	7-AI$(H_2O)_2$	7-AI	7-AI$(H_2O)_1$	7-AI$(H_2O)_2$
A (MHz)	3885	1772	1428	3891	1744	1394
B (MHz)	1707	1395	863	1652	1326	827
C (MHz)	1186	782	541	1161	758	524
ΔI (amu Å^2)	0.00	−0.98	−5.56	−0.53	−3.89	−9.19
N_1C_2	138.4	138.2	138.3	134.2	134.2	134.1
C_2C_3	139.4	139.2	139.0	142.0	141.8	141.8
C_3C_{3a}	141.6	141.6	141.7	146.6	146.5	146.2
$C_{3a}C_{7a}$	145.6	144.8	144.8	136.4	136.5	136.7
$C_{7a}N_1$	132.9	133.9	134.1	142.7	143.2	143.4
$C_{3a}C_4$	139.2	139.4	139.5	143.8	143.7	143.6
C_4C_5	140.4	140.2	140.0	140.5	140.8	141.0
C_5C_6	138.7	139.0	139.0	138.6	138.5	138.3
C_6N_7	135.7	135.2	135.2	140.8	140.5	140.4
N_7C_{7a}	136.1	136.0	135.8	137.4	137.3	137.1
N_7H_7	101.6	103.1	104.4	101.3	102.1	103.0
O_8H_{8a}	⋯	98.8	100.0	⋯	97.7	98.5
O_8H_{8b}	⋯	96.3	96.3	⋯	96.3	96.3
H_7O_8	⋯	186.2	⋯	⋯	198.6	⋯
N_1H_{8a}	⋯	186.7	174.8	⋯	199.0	186.3
$N_7H_7O_8$	⋯	141	⋯	⋯	143	⋯
$N_1H_{8a}O_8$	⋯	145	168	⋯	145	168
$N_7H_7O_8H_{8b}$	⋯	116	147	⋯	109	125
H_7O_9	⋯	⋯	170.3	⋯	⋯	180.8
$N_1H_7O_9$	⋯	⋯	168	⋯	⋯	176
$N_1H_{8a}O_8H_{8b}$	⋯	⋯	−120	⋯	⋯	−134
O_8H_{9a}	⋯	⋯	168.2	⋯	⋯	175.3
$O_8H_{9a}O_9$	⋯	⋯	164	⋯	⋯	163

A. Structures of the 1*H* tautomers

The RICC2 calculated rotational constants and the relevant structural parameters are compiled in Table II. Due to the above described symmetry constraint, the inertial defect ΔI of the ground state of the 1*H* tautomer is calculated to be exactly 0. The same is true for the electronically excited state of 1-*H*-7-azaindole, although no symmetry constraints were made. The slightly negative inertial defect of the cyclic 7-azaindole$(H_2O)_1$ cluster (−1.04 amu Å^2) can be traced back to the out-of-plane position of the hydrogen atom 8*b* (cf. Fig. 1) of the water moiety. On the other hand, the inertial defect of the cyclic 7-azaindole$(H_2O)_2$ cluster (−6.68 amu Å^2) is larger than expected by the two out-of-plane hydrogen atoms of the two water moieties. The experimental rotational constants, given in parentheses, show that the observed tautomer is, indeed, the 1*H*-7-azaindole, both for the monomer and its $n=1,2$ water clusters (compare also for Table II, in which the geometry and rotational constants of the 7*H* tautomer are given).

While the effect of water cluster formation on the geometry of the monomer in the electronic ground state is small, there are large structural effects in the electronically excited state. The change in the azaindole monomer geometry upon electronic excitation can be described as a general increase in the mean bond length in the pyrrole and the pyridine moieties. However, in the 7-azaindole-water clusters, the distortion of the two rings is very irregular. This is, of course, a consequence of the different natures of the observed electronically excited state: L_b in the case of the monomer and L_a for both 7-azaindole-water clusters.

The hydrogen bond strength in the $n=1$ and 2 water clusters of 7-azaindole increases upon electronic excitation as can be seen from the H_1O_8 and the N_7H_{8a} bond lengths in Table II. While for the $n=1$ cluster, the sign of the dihedral angle, which describes the out-of-plane position of the *exo*-hydrogen atom, has no influence on the geometry (the forms with the hydrogen above or below the plane are enantiomers), there exist several arrangements for the $n=2$ cluster. The most stable conformer has one hydrogen atom above (*u*), the other below (*d*) the aromatic plane (*ud*). Other rotamers (*du*,*dd*,*uu*) are slightly higher in energy. Furthermore, the OH bond lengths of the water moiety (or moieties in the case of the $n=2$ cluster) are involved in the hydrogen bond increase, while the *exo*hydrogens remain at the equilibrium value of an isolated water molecule.

B. Structures of the 7*H* tautomers

While for the 1*H* tautomers, the structures in the ground and electronically excited states were found to be planar at RICC2 level, we encounter an out-of-plane structure for the

Downloaded 24 Apr 2012 to 134.99.152.12. Redistribution subject to AIP license or copyright; see http://jcp.aip.org/about/rights_and_permissions

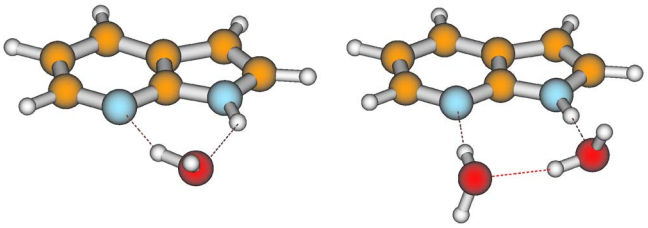

FIG. 2. (Color online) Optimized ground state structure of 7-Azaindole $(H_2O)_1$ and 7-Azaindole $(H_2O)_2$ from the RICC2/TZVP calculations.

electronically excited state of 7*H*-7-azaindole (cf. Table III) with an inertial defect of $\Delta I = -0.53$ amu Å^2. The N_7 and H_7 atoms are tilted out of the aromatic plane (dihedral $C_4C_5C_6N_7 = -7°$ and $C_5C_6N_7H_7 = 162°$), resulting in a pyramidal structure. The lowest electronically excited state for 7*H*-7-azaindole and also for its $n=1,2$ water clusters is the L_a state, in contrast to the 1*H* tautomers. This can also immediately be seen by the similar excited state structural parameters of the monomer and those of the monomer moiety in the clusters.

In contrast to the 1*H*-7-azaindole water clusters, the hydrogen bond strength in the 7*H*-tautomers decreases upon electronic excitation, which can be seen by inspection of the respective hydrogen bond lengths in Table III. Both the azaindole-$(H_2O)_1$ and the azaindole-$(H_2O)_2$ structures in their electronic ground states are depicted in Fig. 2.

C. Relative energies of the tautomers and their water clusters

Table IV shows the relative RICC2 energies of the stationary points for both tautomers in the ground and the first electronically excited singlet states. Zero-point-energy(ZPE) corrections have been made for the ground state by a normal mode analysis at the same level of theory by using analytical second derivatives of the potential energy[31] and for the excited state by numerical differentiation of the energy gradients.

The 1*H* tautomer is the most stable one in the electronic ground state, both for the 7-azaindole monomer and for its water clusters, while this order is reversed in the excited state. Here, the 7*H* tautomer is stabilized by more than 10 000 cm^{-1} compared to the 1*H* tautomer. Like in the ground state, the energy difference between the two tautomers decreases with increasing cluster size.

The last two columns of Table IV contain the RICC2 binding energies of the water clusters of both the 1*H* and the 7*H* tautomers, which are defined by

$$\Delta E_{\text{stab.}} = (E_{\text{AI}(H_2O)_1} + \text{ZPE}_{\text{AI}(H_2O)_1}) - (E_{\text{AI}} + \text{ZPE}_{\text{AI}}) - (E_{(H_2O)_1} + \text{ZPE}_{H_2O}). \quad (1)$$

No correction for the basis set superposition error was made. For the 1*H* tautomer and its clusters, the stabilization energy in the electronically excited state is larger than that in the ground state, while this order is reversed for the 7*H* tautomers. The binding energy of the first water in the 1:1 cluster of 1*H* tautomer amounts to 63 kJ mol^{-1}, the binding energy in the 1:2 cluster is found to be 107 kJ mol^{-1} in their electronic ground states.

Excitation energies (RICC2) to the lowest excited π-π singlet state of the 1*H* tautomer are calculated from the data of Table IV to be 33 964, 33 288, and 32 380 cm^{-1} for the monomer, and the $n=1,2$ water clusters, respectively, in quite good agreement with the experimental values (cf. Sec. III D). For the 7*H* tautomer, the respective electronic excitation energies are 19 036, 21 149, and 22 678 cm^{-1}. More exact values for the electronically excited states can be obtained by using the DFT/MRCI method of Grimme and Waletzke,[28] as will be shown in the following subsection.

D. Electronic excitation energies and dipole moments

The vertical and adiabatic excitation energies, the orientation of the transition dipole moment (TDM), and the ground and excited state permanent dipole moments of azaindole and the $n=1,2$ water clusters have been calculated by using the DFT/MRCI method of Grimme and Waletzke.[28] Since, by comparison to the experimental rotational constants, the RICC2/TZVP optimized geometry has been shown to be the most reliable one, the adiabatic excitation energies have been determined in this geometry and were corrected by the ZPE calculated at the same level of theory. Exceptions are indole, indole-water, and the azaindole-ar cluster, for which the vibrational frequencies were calculated at the B3-LYP/TZVP level for the ground state and TD-B3-LYP/TZVP for the excited state. Compared to RICC2/TZVP calculated ZPE contributions, a deviation of 500 cm^{-1} at most can be expected. The permanent dipole moments are

TABLE IV. Absolute energies (hartrees), relative energies $\Delta E_{\text{rel.}}$ (cm^{-1}) of the 1*H* and 7*H* tautomers of 7-azaindole and its $n=1$, 2 water clusters, and binding energies of the 7*H* and 1*H*-7-azaindole-water clusters $\Delta E_{\text{stab.}}$ (cm^{-1}) calculated at the RICC2/TZVP level of theory.

					$\Delta E_{\text{stab.}}$	
		1*H*-7azaindole	7*H*-7azaindole	$\Delta E_{\text{rel.}}$	1*H*	7*H*
S_0	7-AI	−378.765 022 017	−378.745 328 920	4 322	⋯	⋯
	$7AI(H_2O)_1$	−455.045 646 664	−455.030 762 679	3 267	5 261	6 316
	$7AI(H_2O)_2$	−531.319 253 076 0	−531.306 933 484	2 703	8 982	10 600
S_1	7-AI	−378.609 883 617 6	−378.658 204 536 1	−10 605	⋯	⋯
	$7AI(H_2O)_1$	−454.893 508 131 3	−454.929 376 911 2	−7 872	5 919	3 186
	$7AI(H_2O)_2$	−531.171 171 169 1	−531.203 058 780 5	−6 998	10 530	6 924

Downloaded 24 Apr 2012 to 134.99.152.12. Redistribution subject to AIP license or copyright; see http://jcp.aip.org/about/rights_and_permissions

given in Cartesian components (in debye) of the principal inertial system; the TDM orientations are given as the angle θ between the projection vector of the TDM on the inertial ab plane and the a axis and as the angle ϕ between the TDM and the inertial c-axis,

$$\mu_a = \mu \sin\phi \cos\theta,$$

$$\mu_b = \mu \sin\phi \sin\theta, \tag{2}$$

$$\mu_c = \mu \cos\phi.$$

Table V shows a very good agreement of the calculated absolute adiabatic excitation energies (corrected for ZPE at the RICC2/TZVP level) with the experimentally determined electronic origins of 7-azaindole and the $n=1,2$ water clusters. The permanent dipole moment of the excited state of 7-azaindole has been calculated to be 2.1 D, in good agreement with the value of 2.33 D, which was obtained by Kang *et al.* from a Stark measurement.[15] This value is typical for the dipole moment of a L_b state. The corresponding value for the ground state dipole moment is 1.63 D, compared to 1.45 D from Ref. 15. For the TDM orientation of 7-azaindole, the angle of the transition moment with the inertial a axis is predicted to be +20.5 °, while experimentally determined values of −20 ° (Ref. 13) and −14 ° (Ref. 32) have been reported. A value of −20 ° means an orientation nearly parallel to the N_1C_{7a} bond in Fig. 1. The reason for this discrepancy between experiment and theory is still not clear and is subject to further investigations.

For comparison, we also calculated the vertical and adiabatic spectra of indole,[33] the gpy(out) conformer of tryptamine,[34] and their water clusters,[34,35] for which the relevant experimental informations (i.e., structure, dipole moments, and TDM orientation) are also available. The results are compiled in Table V. Most experimental investigations of the TDM using rotationally resolved electronic spectroscopy yield only the absolute values, since the observed intensities in the spectra depend on the squares of the transition moments in Eq. (2). For all cases, in which apart from the absolute value, the orientation of the TDM is also available from the experiment, the DFT/MRCI method yields the correct sign for the angle. Even the absolute values of the angle are in good agreement with the experimentally determined angles. For tryptamine, the sign of the TDM angle has been determined from comparison of the TDM angle in the gpy(out) conformer of tryptamine to the values from a hitherto unpublished rotationally resolved electronic tryptamine-Ar spectrum. Also, the adiabatic excitation energies and excited state dipole moments are in very good agreement with the experiment.

The lowest electronically excited state of the 7-AI$(H_2O)_1$ cluster has a much higher permanent dipole moment (5.29 D) than the monomer, owing to the fact that this state is, indeed, the L_a state. The same holds for the 7-AI$(H_2O)_2$ cluster. Also, the orientation of the TDM is in agreement with this assignment of the excited states. The large spectral redshifts of the excitation energies upon cluster formation (−1290 cm^{-1} for $n=1$ and 2000 cm^{-1} for $n=2$) can, therefore, be traced back to the fact that the S_1 state in the case of the monomer can be identified as L_b, while it is the L_a state for the water clusters.

IV. CONCLUSIONS

RICC2/TZVP optimizations of the geometries of the two tautomers of 7-azaindole and its $n=1$ and 2 water clusters have been performed. The comparison to experimental rotational constants show that the observed tautomer is the 1H tautomer, which is also found to be the most stable one in the electronic ground state. Nearly quantitative agreement for the ground and excited state rotational constants is found at this level of theory. The agreement is even too close, considering the fact that the experimental rotational constants are vibrationally averaged B_0 values, while the calculated constants are equilibrium B_e values.

Electronic excitation of 7-azaindole to the S_1 state of the 1H tautomer reverses this energetic ordering, 7H now being the more stable one. The lowest π-π^* singlet state (S_1) in the case of the 1H tautomer mainly has L_b character and the S_2 state mainly has L_a character, while for the 7H-7-azaindole, the L_a state is the lowest excited π-π^* singlet state.

Water complexation of 7-azaindole with one and two water molecules stabilizes the more polar L_a state to such an extent, which for the more stable 1H tautomer, the lowest excited singlet state is no longer the L_b but the L_a state. This state is the experimentally observed one, as can be seen by comparison of the rotational constants of both excited states with the experimentally determined parameters.

The orientation of the TDM in the monomer of 7-azaindole has been determined to be +20°, in contrast to the experimental value of −20 °. Further experimental investigations by using other isotopomers and eventually clusters of noble gases, which change only the inertial axis system but not the direction of the TDM, are necessary to decide which of the orientations is the correct one.

Adiabatic and vertical excitation energies and orientations of the TDMs have been calculated at the RICC2/TZVP, the TDDFT/TZVP with the B3-LYP functional, and at the DFT/MRCI level of theory with BH-LYP KS orbitals. For RICC2 and TDDFT, the structures optimized at the same level of theory were employed, and for DFT/MRCI, we used the RICC2 optimized structures. Table VI compares the excitation energies and Table VII compares the TDM orientations using the above methods. Grimme and Parac[36] concluded for excited states of large π systems that TDDFT has not only substantial discrepancies for the description of Rydberg and charge transfer states, where it suffers from the wrong asymptotic behavior of the exchange-correlation functionals, but also for low-lying valence states. Comparison of the RICC2 and DFT/MRCI calculations with the experimental values shows that both methods behave nearly equally well, with a dramatic difference in the computational cost for the two methods. The norm of the single excitation cluster operator $\|T1\|$, which is a measure of the single reference character of the respective state,[22] shows that both the L_a and the L_b states are predominantly single reference states. Therefore, deviations due to large contributions of ionic

Downloaded 24 Apr 2012 to 134.99.152.12. Redistribution subject to AIP license or copyright; see http://jcp.aip.org/about/rights_and_permissions

TABLE V. DFT/MRCI calculated vertical and adiabatic singlet excitation energies ($\nu_{\mathrm{el.}}$) with the electric dipole transition oscillator strengths in the length representation $f(r)$ displayed in parentheses, dipole moment components ($\mu_g, g=a,b,c$) of the excited state, their absolute values ($|\mu|$), the angle between the projection vector of the TDM on the ab plane and the a axis (θ), and the angle between the TDM and the c axis (ϕ) of 1*H*-7-azaindole and the $n=1$, 2 water clusters. Adiabatic excitation energies are ZPE corrected. Values for indole, tryptamine, and their water cluster are given for comparison. The references in the first column refer to the experimental values of the respective molecule/cluster.

		Vertical		Adiabatic	
		S_1	S_2	S_1	Expt.
7-AI[a]	$\nu_{\mathrm{el.}}$	36 396(0.093)	38 186(0.135)	35 013(0.100)	34 630.74
	μ_a			1.91	2.23
	μ_b			0.79	0.55
	$\|\mu\|$			2.1	2.23
	θ			+20.5	−20
	ϕ			+90	90
7-AI$(H_2O)_1$[b]	$\nu_{\mathrm{el.}}$	36 059(0.066)	36 604(0.148)	33 214(0.100)	33 340.43
	μ_a			2.69	⋯
	μ_b			4.46	⋯
	μ_c			0.92	⋯
	$\|\mu\|$			5.29	⋯
	θ			+18.8	±27
	ϕ			+89.4	±86
7-AI$(H_2O)_2$[b]	$\nu_{\mathrm{el.}}$	35 577(0.043)	36 088(0.162)	32 751(0.087)	32 632.10
	μ_a			0.97	⋯
	μ_b			4.94	⋯
	μ_c			0.36	⋯
	$\|\mu\|$			5.05	⋯
	θ			33.7	±34
	ϕ			87.1	±74
7-AI-Ar[c]	$\nu_{\mathrm{el.}}$			35 082(0.086)	34 606
	μ_a			1.63	⋯
	μ_b			0.60	⋯
	μ_c			0.69	⋯
	$\|\mu\|$			1.87	⋯
	θ			+77	±77
	ϕ			+76	±77
Indole[d]	$\nu_{\mathrm{el.}}$	36 957(0.027)	40 154(0.181)	35 147(0.047)	35 231
	μ_a			1.44	1.56
	μ_b			0.98	1.01
	$\|\mu\|$			1.74	1.86
	θ			+40	+38.3
	ϕ			+90	+90
Indole$(H_2O)_1$[e]	$\nu_{\mathrm{el.}}$	36 806(0.027)	39 310(0.160)	35 121(0.054)	35 100
	μ_a			3.21	3.90
	μ_b			1.68	0.9
	$\|\mu\|$			3.62	4.0
	θ			+81	±90
	ϕ			+90	±90
Tryptamine[d]	$\nu_{\mathrm{el.}}$	36 900(0.022)	39 170(0.136)	34 841(0.047)	34 916
	μ_a			0.03	0.10
	μ_b			1.00	1.26
	μ_c			0.61	0.46
	$\|\mu\|$			1.17	1.25
	θ			+77	+72
	ϕ			+4	+14
Tryptamine$(H_2O)_1$[d]	$\nu_{\mathrm{el.}}$	36 845(0.019)	38 947(0.130)	34 872(0.021)	34 957
	μ_a			1.54	⋯
	μ_b			1.04	⋯

Downloaded 24 Apr 2012 to 134.99.152.12. Redistribution subject to AIP license or copyright; see http://jcp.aip.org/about/rights_and_permissions

TABLE V. (*Continued.*)

	Vertical		Adiabatic	
	S_1	S_2	S_1	Expt.
μ_c			1.02	⋯
$\|\mu\|$			2.11	⋯
θ			+75	±66
ϕ			+19	±10

[a]Reference 13.
[b]Reference 16.
[c]Reference 32.
[d]Reference 35.
[e]Reference 33.
[f]Reference 34.

states, that are resposible for the problems in the description of polycyclic aromatic hydrocarbons using TDDFT (Ref. 37) are small in the present case, as has been shown previously for some aromatic hydrocarbons[28] and for different conformers of tryptamine.[34] While TDDFT is formally an exact method (although for practical applications, the functionals have to be approximated), DFT/MRCI lacks this rigid formalism but is a very successful semiempirical approach. DFT/MRCI is able to reproduce accurately not only experimental TDMs but also adiabatic excitations energies, in cases were TDDFT even fails to give the correct order of the valence states. Very recently, Grimme and Neese[38] presented a double-hybrid density functional ansatz, which is capable of correctly describing the energetic ordering of the L_a and L_b states of polycyclic aromatic hydrocarbons in the framework of TDDFT.

Table VII shows that despite the fact that the adiabatic excitation energies from the TDDFT calculations even do not reproduce the experimental ordering correctly, the TDM orientations for the corresponding states in the TDDFT, RICC2, and DFT/MRCI calculations are very similar. As a guidance, Platts nomenclature for the electronically excited states are added, although they provide only a rough description in this unsymmetric molecules. All calculations agree that the lowest two states of 7-azaindole and its water clusters are of L_a or L_b type.

The results, presented in the present work, show that the improvement of the adiabatic excitation energies by combining DFT and CI methods, which is due to "the use of information about dynamical electron correlation from DFT and the treatment of nondynamical effects by CI methods" (citation from Ref. 28) is substantial in the case of 7-azaindole and its water clusters. Another important effect, which improves the performance of DFT/MRCI, is the use of the BH-LYP functional, with a high amount of Hartree–Fock exchange. Regarding the large computational cost of the CC method, the use of KS orbitals as single electron basis for MRCI presents an attractive alternative. Nevertheless, the method strongly relies on the correctness of the excited state structures. Therefore, DFT/MRCI based on RICC2 optimized structures leads to results closer to the experimental ones (especially for the excitation energies) than based on TDDFT optimized structures. Since the great part of the attractiveness of the DFT/MRCI method is based on the fact

TABLE VI. Comparison of RICC2, DFT/MRCI, and TDDFT calculated vertical and adiabatic singlet excitation energies (cm^{-1}) of the two lowest excited singlet state(s). Adiabatic excitation energies are ZPE corrected at the level of the optimization. For RICC2 calculations, the T1 norm, which is a measure of the contribution of a single reference character of this state, is given in parentheses.

	RICC2		DFT/MRCI		TDDFT		Expt.	
S_n	Vertical	Adiabatic	Vertical	Adiabatic	Vertical	Adiabatic	Ref. 39[a]	Ref. 16[b]
				7-AI				
S_1	38 852 (92)	34 049(91)	36 396	35 013	37 321	33 169	34500	34 631
S_2	40 317 (92)	⋯	38 186	⋯	39 433	38 044	36100	⋯
				7-AI$(H_2O)_1$				
S_1	37 764 (92)	33 390(92)	36 059	33 214	35 831	31 869	⋯	33 340
S_2	38 982 (92)	⋯	36 604	⋯	38 958	⋯	⋯	⋯
				7-AI$(H_2O)_2$				
S_1	37 083 (92)	32 500(92)	35 577	32 751	35 167	30 593	⋯	32 632
S_2	38 704 (92)	⋯	36 088	⋯	38 718	⋯	⋯	⋯

[a]Ar matrix data.
[b]Molecular beam data.

Downloaded 24 Apr 2012 to 134.99.152.12. Redistribution subject to AIP license or copyright; see http://jcp.aip.org/about/rights_and_permissions

TABLE VII. Comparison of RICC2, DFT/MRCI, and TDDFT calculated TDM orientations of the two lowest excited singlet states.

	RICC2[a]			DFT/MRCI			TDDFT			Expt.		
S_n	Type	θ	ϕ	Type	θ	ϕ	Type	θ	ϕ	Type	θ	ϕ
						7-AI						
S_1	L_b	±27.0	90.0	L_b	+20.5	90.0	L_a	−33.9	90.0	L_b	±20	90
S_2	L_a	±30.0	90.0	L_a	−37.9	90.0	L_b	+21.5	90.0			
						7-AI$(H_2O)_1$						
S_1	L_a	±14.6	±89.7	L_a	+18.8	+89.4	L_a	+17.1	+89.4	L_a	±27	±86
S_2	L_b	±52.4	±89.2	L_b	+75.0	+88.6	L_b	+69.9	+89.8			
						7-AI$(H_2O)_2$						
S_1	L_a	±28.5	±87.5	L_a	+33.7	+87.1	L_a	+47.8	+89.2	L_a	±34	±74
S_2	L_b	±69.3	±89.3	L_b	+87.5	+87.4	L_b	+59.9	+88.3			

[a]No direction of the TDM for RICC2 can be given, since RICC2 is a nonvariational method and the left and right transition moments are different. Transition strengths are obtained as a symmetrized combinations of both moments. Thus, only transition strengths are available, and the direction information of the transition moment is lost.

that it is used with computational cheap TDDFT optimized structures, a considerable improvement can be expected from the implementation of DFT/MRCI gradients.

ACKNOWLEDGMENTS

This work has been performed in the SFB 663 TP A2, Universität Düsseldorf and was printed upon its demand with financial support from the Deutsche Forschungsgemeinschaft. We thank Christel Marian for helpful discussions. Granted computing time at Universität-srechenzentrum Köln and at the Austrian Grid network and computational facilities of the Johannes Kepler Universität Linz are gratefully acknowledged.

[1] A. Held and D. W. Pratt, J. Am. Chem. Soc. **115**, 9708 (1993).
[2] A. Bach and S. Leutwyler, J. Chem. Phys. **112**, 560 (2000).
[3] A. Kyrychenko and J. Waluk, J. Phys. Chem. A **110**, 11958 (2006).
[4] M. S. Gordon, J. Phys. Chem. **100**, 3974 (1996).
[5] M. Shukla and P. Mishra, Chem. Phys. **230**, 187 (1998).
[6] A. C. Borin and L. Serrano-Andrés, Chem. Phys. **262**, 253 (2000).
[7] L. Serrano-Andrés and A. C. Borin, Chem. Phys. **262**, 267 (2000).
[8] R. Casadesús, M. Moreno, and J. M. Lluch, Chem. Phys. **290**, 319 (2003).
[9] A. Fernández-Ramos, Z. Smedarchina, W. Siebrand, and M. Z. Zgierski, J. Chem. Phys. **114**, 7518 (2001).
[10] A. Nakajima, M. Hirano, R. Hasumi, K. Kaya, H. Watanabe, C. C. Carter, J. Williamson, and T. A. Miller, J. Phys. Chem. A **101**, 392 (1999).
[11] H. Yokoyama, H. Watanbe, T. Omi, S. Ishiuchi, and M. Fujii, J. Phys. Chem. A **105**, 9366 (2001).
[12] R. Brause, D. Krügler, M. Schmitt, K. Kleinermanns, A. Nakajima, and T. A. Miller, J. Chem. Phys. **123**, 224311 (2005).
[13] M. Schmitt, C. Ratzer, K. Kleinermanns, and W. L. Meerts, Mol. Phys. **102**, 1605 (2004).
[14] R. Brause, M. Schmitt, D. Spangenberg, and K. Kleinermanns, Mol. Phys. **102**, 1615 (2004).
[15] C. Kang, J. T. Yi, and D. W. Pratt, Chem. Phys. Lett. **423**, 7 (2006).
[16] T. B. C. Vu, I. Kalkman, W. L. Meerts, Y. N. Svartsov, and M. Schmitt, J. Chem. Phys. **128**, 214311 (2008).
[17] R. Ahlrichs, M. Bär, M. Häser, H. Horn, and C. Kölmel, Chem. Phys. Lett. **162**, 165 (1989).
[18] A. Schäfer, C. Huber, and R. Ahlrichs, J. Chem. Phys. **100**, 5829 (1994).
[19] O. Treutler and R. Ahlrichs, J. Chem. Phys. **102**, 346 (1995).
[20] F. Furche and R. Ahlrichs, J. Chem. Phys. **117**, 7433 (2003).
[21] A. D. Becke, J. Chem. Phys. **98**, 5648 (1993).
[22] C. Hättig and F. Weigend, J. Chem. Phys. **113**, 5154 (2000).
[23] C. Hättig and A. Köhn, J. Chem. Phys. **117**, 6939 (2002).
[24] C. Hättig, J. Chem. Phys. **118**, 7751 (2002).
[25] C. Peng and H. B. Schlegel, Isr. J. Chem. **33**, 449 (1994).
[26] M. J. Frisch, G. W. Trucks, H. B. Schlegel *et al.*, GAUSSIAN 03, revision a.1, Gaussian, Inc., Pittsburgh, PA, 2003.
[27] T. Helgaker, Chem. Phys. Lett. **182**, 503 (1991).
[28] S. Grimme and M. Waletzke, J. Chem. Phys. **111**, 5645 (1999).
[29] A. D. Becke, J. Chem. Phys. **98**, 1372 (1993).
[30] C. Lee, W. Yang, and R. Parr, Phys. Rev. B **37**, 785 (1988).
[31] H. Horn, H. Weiss, M. Häser, M. Ehrig, and R. Ahlrichs, J. Comput. Chem. **12**, 1058 (1991).
[32] C. Kang, J. T. Yi, and D. W. Pratt, J. Chem. Phys. **123**, 094306 (2005).
[33] T. M. Korter, D. W. Pratt, and J. Küpper, J. Phys. Chem. A **102**, 7211 (1998).
[34] M. Schmitt, R. Brause, C. Marian, S. Salzmann, and W. L. Meerts, J. Chem. Phys. **125**, 124309 (2006).
[35] C. Kang, T. M. Korter, and D. W. Pratt, J. Chem. Phys. **122**, 174301 (2005).
[36] S. Grimme and M. Parac, ChemPhysChem **3**, 292 (2003).
[37] M. Parac and S. Grimme, Chem. Phys. **292**, 11 (2003).
[38] S. Grimme and F. Neese, J. Chem. Phys. **127**, 154116 (2007).
[39] P. Ilich, J. Mol. Struct. **354**, 37 (1995).

Downloaded 24 Apr 2012 to 134.99.152.12. Redistribution subject to AIP license or copyright; see http://jcp.aip.org/about/rights_and_permissions